Journal Name

ARTICLE

Interfacial crowding of nanoplatelets in co-continuous polymer blends: assembly, elasticity and structure of the interfacial nanoparticle network

Received 00th January 20xx,
Accepted 00th January 20xx

DOI: 10.1039/x0xx00000x

www.rsc.org/

R. Altobelli, [§a] M. Salzano de Luna*[§a,b] and G. Filippone*[a]

The sequence of events that leads to the interfacial crowding of plate-like nanoparticles in co-continuous polymer blends is investigated through a combination of morphological and rheological analyses. Very low amounts (~0.2 vol%) of organo-modified clay are sufficient to suppress phase coarsening in a co-continuous polystyrene/poly(methyl methacrylate) blend, while lower particle loading allows for a tuning of the characteristic size of the polymer phases at the µm-scale. In any case, an interfacial network of nanoparticles eventually forms driven by the preferred polymer-polymer interface. The elastic features and stress-bearing ability of this peculiar nanoparticle assembly are studied in detail by means of a descriptive two-phase viscoelastic model, which allows to isolate the contribution of the filler network. The role of the co-continuous matrix in driving the space arrangement of the nanoparticles is emphasized by means of comparative analysis with systems based on the same polymers and nanoparticles, but in which the matrix is either a pure polymer or a blend with drop-in-matrix morphology. The relaxation dynamics of the interfacial network were found not to depend on the matrix microstructure, which instead substantially affects the assembly of the nanoplatelets. When the host medium is co-continuous, the particles align along the preferred polymer-polymer interface, percolating at very low amount (~0.17 vol%) and prevalently interacting edge-to-edge. The stress bearing ability of such a network is much higher than in case of matrix based on homogeneous polymer or drop-in-matrix blend, but its elasticity has low sensitivity to the filler content.

Introduction

The ability of fine particles to stabilize fluid–fluid interfaces has attracted considerable attention since its discovery at the beginning of last century.[1,2] Since then, the interfacial adsorption of micro- or nanoparticles has been widely exploited to control the phase morphology of low-viscosity emulsions, while less attention has been devoted to their high-viscosity counterparts, viz. immiscible polymer blends. Actually, the underlying physics does not depend on the nature of the fluids, which mostly dictate the timescales of the phenomena.[3] Nowadays, the ability of nano-sized particles in gluing polymer drops to form clusters, preserving non-spherical domains and promoting stable co-continuous morphologies in polymer blends is widely recognized.[4] As a result, the interest is now mainly directed towards the use of the filler as a clever tool for manipulating the blend morphology at the micron scale.[5] Governing the microstructure of polymers blends is highly attractive from a technological pint of view. The reason is that the macroscopic properties of this class of materials are strictly related to the small-scale arrangement of the polymer phases.[6] The possibility of a fine tuning of the blend morphology is particularly intriguing in case of co-continuous polymer blends, in which the mutual interpenetration of the phases can result in a synergistic combination of the properties of the constituents. The addition of nanoparticles to co-continuous blends is known to be effective in suppressing phase coarsening,[7-9] but the spectrum of possibilities offered by a clever use of the filler is actually much wider. Recently, the addition of nanoparticles to co-continuous blends has been ingeniously exploited to promote hierarchical structures,[10] to enhance the heat deflection temperature of bio-based polymers,[11] to improve the mechanical properties of engineering plastics,[12] or to refine the dispersion of nanoparticles in polymer matrices.[13] Besides exploiting the ability of nanoparticles to alter the blend morphology, one can refer to the other side of the coin by profiting from the phase-separated morphology of the matrix to control the space arrangement of the filler. In principle, the continuous liquid-liquid interface can be used as a template for a controlled three-dimensional assembly of nanoparticles, opening new routes for a bottom-up material design. Some notable results have been obtained in systems based on low-viscosity fluids,[14-15] but a full understanding of the complex interplay between fluid evolution and nanoparticles self-assembly is still far from being reached, especially in the case of high viscosity polymer blends. An important step in this direction is due to Macosko and co-workers, who monitored in real time the interface dynamics in bicontinuous,

[a] *Dipartimento di Ingegneria Chimica, dei Materiali e della Produzione Industriale (INSTM Consortium – UdR Naples), University of Naples Federico II, P.le Tecchio 80, 80125 Naples, Italy.*
[b] *Institute for Polymers, Composites and Biomaterials, National Research Council of Italy, P.le E. Fermi 1, 80055, Portici (NA), Italy.*
E-mail: martina.salzanodeluna@unina.it; gfilippo@unina.it
§ These authors contributed equally.
† Electronic Supplementary Information (ESI) available: Procedure for the building of the master curve of G' and resulting shift factors. See DOI: 10.1039/x0xx00000x

interfacially jammed, emulsion gels (bijels) to access the changes in the interfacial particle coverage.[16] The authors shed light on the sequence of events that lead to the formation of the bijel, which results from the shrinking of the liquid-liquid interface until interfacial particle jamming. However, extending their conclusions to inherently immiscible blends of highly viscous polymers is not straightforward. Different scenarios are also expected when non-spherical particles are considered. Plate-like fillers, indeed, better adapt to the polymer–polymer interface and, if provided with sufficient bending stiffness, they can constrain the evolution of the fluid phases without the need of interfacial jamming, which is instead required for spheres. Moreover, the strength of the interfacial network of nanoparticles, ultimately responsible for the mechanical stability of the material in the melt state, has not been studied in detail. In this work we address these issues, investigating the dynamics of assembly, the elasticity and the structure of interfacial networks of clay nanoplatelets in co-continuous blends of polystyrene (PS) and poly(methyl methacrylate) (PMMA). We use a combination of morphological analyses and rheological investigations to prove the generality of the mechanism of morphology stabilization by interfacial crowding of nanoparticles, which keeps working in spite of the high viscosity of the liquid phases and the plate-like shape of the nanoparticles. The structure and stress-bearing ability of the resulting interfacial network of nanoparticles are investigated through a descriptive viscoelastic model that enables to isolate the elastic contribution of the nanoparticle network from that of the host matrix. The effect of the co-continuous morphology of the host matrix is highlighted through a comparative analysis with systems based on the same polymers and nanoparticles as used here, but in which the matrix is either a single polymer or a drop-in-matrix blend. This allows to emphasize the role of the multiphase nature of the host medium in driving the nanoparticle assembly.

Experimental

The polystyrene (PS, trade name Edistir® 2982, by Polimeri Europa) has glass transition temperature T_g=100°C, density ρ=1.04 g cm^{-3}. The poly(methyl methacrylate) (PMMA, trade name Optix® CA-51, by Plaskolite, Inc.) has T_g=110°C, ρ=1.18 g cm^{-3}. The filler is a montmorillonite modified with dimethyl dihydrogenated tallow quaternary ammonium salt (Cloisite® 15A by Southern Clay Products, Inc.), having organic content ~43 wt% and ρ=1.66 g cm^{-3}. Previous studies showed that Cloisite® 15A accumulates at the polymer-polymer interface when dispersed in PS-PMMA blends.[17]

Unfilled and filled PS/PMMA blends at 55/45 weight ratio were prepared by melt compounding the constituents using a recirculating, conical twin screw micro-compounder (Xplore MC 15 by DSM). The polymers and the filler, dried overnight under vacuum at T=90°C, were loaded simultaneously in the mixing apparatus. The extrusions were performed at T=190°C in nitrogen atmosphere at a screw speed of 150 rpm. The residence time was about 5 minutes. The extrudate was granulated, dried again, and finally compression-moulded in the form of disks (diameter 40 mm, thickness ~1.5 mm) for the subsequent rheological and morphological analyses.

The particle loading was accurately estimated for each sample by means of thermogravimetric analyses (TGA, Q5000 by TA Instruments). Tests were carried out small pieces cut from the disks recovered at the end of rheological analyses. The samples were heated at 10°C min^{-1} in nitrogen atmosphere from room temperature up to T=700°C, and the residuals were recorded at T=600°C. The reported values of filler content, expressed in terms of percentage volume fraction of the inorganic fraction, Φ, are averages computed from three independent measurements.

The morphology of the samples was investigated by means of electron microscopy. TEM analyses (Tecnai G2 Spirit Twin T-12 by FEI) were carried out to identify the space arrangement of the nanoplatelets. The samples were ~100 nm-thick slices randomly cut at room temperature from the disks used for rheological analyses by using a Leica EM UC7 ultra-microtome equipped with a diamond knife. SEM analyses (Quanta 200 FEG-SEM by FEI) were performed to study the morphology of the polymer phases. Before observations, the surface of the cryo-fractured samples was etched with formic acid to selectively remove the PMMA phase, and then coated with a 15-nm thick Au/Pd layer using a sputter coating system. The SEM micrographs were analysed to get an estimate of the characteristic size of the PMMA phase, ξ, which was defined as 1/Q, where Q is the interfacial length per unit area. For each samples, several images at different magnifications were analysed by manually detecting the interfacial perimeter.

Rheological tests were performed at T=215°C in dry nitrogen atmosphere using a stress-controlled rotational rheometer (ARG2 by TA Instruments) in parallel-plate configuration. The elastic (G') and viscous (G'') shear moduli were collected by means of time and frequency scans. All the tests were performed at strain amplitudes low enough to be in the linear regime. The latter was evaluated for each sample through preliminary strain amplitude tests.

Results and Discussion

Effects of the nanoparticles on the blend microstructure

All the samples exhibit co-continuous microstructure at the end of the preparation procedure. The morphology of a representative sample at Φ=0.22% is shown in Fig. 1. The characteristic size of the polymeric phases is of the order of few microns. The nanoclay is in the form of intercalated stacks lying at the PS-PMMA interface. The interfacial localization of the selected particles agrees with thermodynamic predictions based on wettability calculations (for details see ESI†, Section S1).[17] The presence of nanoplatelets accumulated at the polymer-polymer interface radically alters the coalescence, breakup and relaxation phenomena on the basis of the development of the microstructure in immiscible polymer blends.[5] The effect of the filler on the initial morphology of the blends is shown in Fig. 2, where the average size of the PMMA domains in the as-prepared samples is reported as a function of filler content. The nanoparticles induce a drastic reduction of ξ, which falls to about one-seventh of its value in the unfilled blend by simply adding 0.22% of nanoclay to the initial

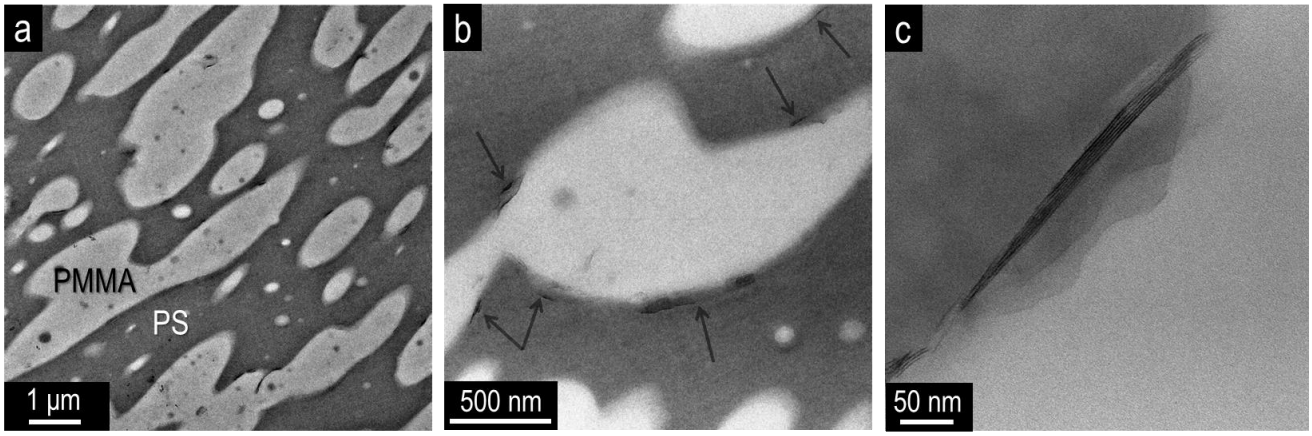

Fig. 1 TEM micrographs of the as-extruded blend at Φ=0.22% at different magnifications. The bright and dark phases are PMMA and PS, respectively. The arrows in (b) indicate the clay lying at the polymer-polymer interface.

polymer mixture. The effect rapidly decreases with Φ, and ξ approaches a limiting value <1 µm. Given that the lateral dimensions of montmorillonite-based nanoclays is of order of 0.5 µm, this value is in line with the prediction by Rafailovich and co-workers, who set that the minimum allowable domain size is of order of the lateral size of a nanoplatelet to avoid energetically unfavourable particle folding.[18]

Nanoparticle-induced refinement is a well-known phenomenon in case of blends with drop-in-matrix morphology.[5] The most convincing arguments invoked to explain the phenomenon in case of interfacially-adsorbed plate-like nanoparticles are coalescence suppression and alteration of the interfacial rheology. The former mechanism assumes that nanoplatelets act as a physical barrier that prevents the direct contact between polymer domains during melt-mixing.[19,20] Regarding interfacial rheology effects, the nanoplatelets provide the interface with a marked viscous and elastic connotation, thus retarding the relaxation phenomena involved in the coarsening process in the melt state.[21,22] Despite the lack of focused studies, the previous mechanisms can be invoked also in case of melt-mixed co-continuous blends, whose microstructure stems from the same basic events occurring in blends with distributed morphology.

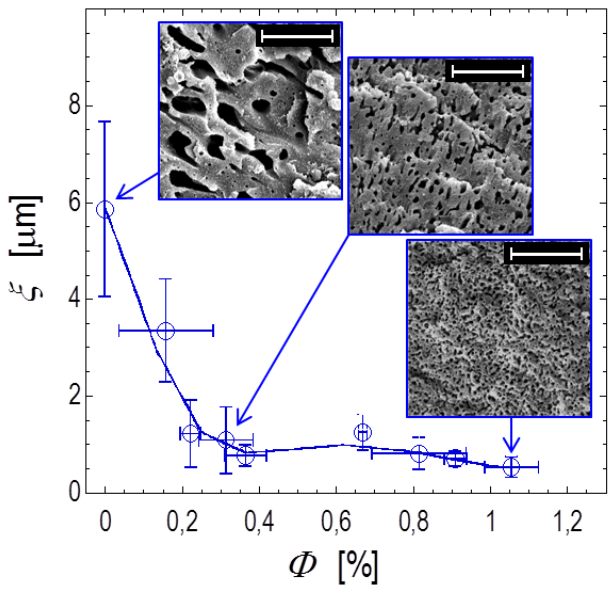

Fig. 2 Average size of the PMMA domains in samples at different filler contents before any thermal annealing treatment. The solid line is a guide for the eye. Representative SEM micrographs of selected as-prepared samples are shown as insets. The scale bars correspond 20 µm.

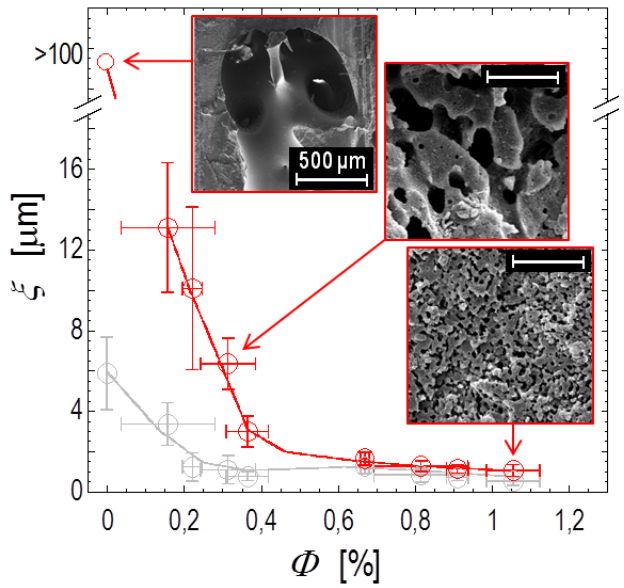

Fig. 3 Average size of the PMMA domains in samples at different filler contents after a 3-hour annealing at *T*=215°C. The data before annealing are also reported for comparison (semi-transparent symbols; same data as in Fig. 2). Solid lines are guides for the eye. Representative SEM micrographs of selected samples are shown as insets. When not indicated, the scale bars correspond to 20 µm.

Besides refining the initial morphology, interfacially-adsorbed nanoparticles are also known to stabilize the co-continuous microstructures against phase coarsening.[7-9,16,23,24] The stabilizing action in the studied system is shown in Fig. 3, where the average size of the PMMA domains in samples at different filler content is reported after a 3-hour annealing at T=215°C. Drastic phase coarsening occurs in the unfilled blend, whose polymer phases resulted completely segregated at the end of the annealing process. The presence of nanoparticles significantly stabilizes the morphology. Two different behaviours can be recognized depending on the filler content. At Φ<0.67% the nanoparticles limit phase coarsening without arresting it, and their ability to do so is proportional to their content. The linear trend at 0.16≤Φ≤0.36% suggests a clever way to control the extent of interface, or equivalently the characteristic size of the polymer phases. The latter indeed can be finely tuned at the micron-scale by simply changing the particle loading and letting the blend to coarsen. Differently, at Φ≥0.67% full morphology stabilization is achieved irrespective of the filler content. Monitoring the viscoelastic moduli during annealing allows to shed light on the origin of morphology stabilization. We focus on G', which is strictly related to the extent and the elastic features of the polymer-polymer interface. The time dependence of G' is reported in Fig. 4 for selected samples below and above the threshold that discriminates between partial (Φ<0.67%) and full (Φ≥0.67%) morphology stabilization. The G' of the unfilled blend decreases during time, eventually reaching a steady state value. The overall elasticity of polymer blends reflects the elasticity of constituents, which is stable in the investigated time window, plus an extra contribution stemming from the polymer-polymer interface. The interfacial tension drives the system towards morphologies characterized by lower interfacial area. As the latter shrinks, the interfacial contribution decreases along with G'. We now consider the filled blends. At Φ≥0.67%, i.e. when the morphology is stable over time, a rapid growth of G' is observed in the early stages of the tests, then the modulus slowly approaches a steady value. Such a behaviour is well known in single-polymer nanocomposites, whose elasticity increases at rest due to space rearrangements of the filler.[25] Now consider the partially stabilized samples at Φ<0.67%. At Φ=0.16 and 0.22%, G' decreases in the very early stages of the test, and then it starts growing. The higher the Φ, the lower the time required for the inversion of the sign of $\partial G'/\partial t$. The behaviour of these partially stabilized samples reminds that of polymer bijels based on spherical particles.[16] Bijels are non-equilibrium structures which form due to the jamming of colloidal particles at the interface between two partially miscible low-viscosity fluids that undergo spinodal decomposition.[26,27] In such systems, the sequence of decrease and growth of $G'(t)$ reflects the succession of interfacial shrinking and particle jamming at the liquid-liquid interface. Here, the liquids are inherently immiscible highly viscous polymers, and the particles are flexible plate-like nanoclays. Despite these substantial differences, the rheological analysis indicates that the mechanism of morphology stabilization is the same. The TEM

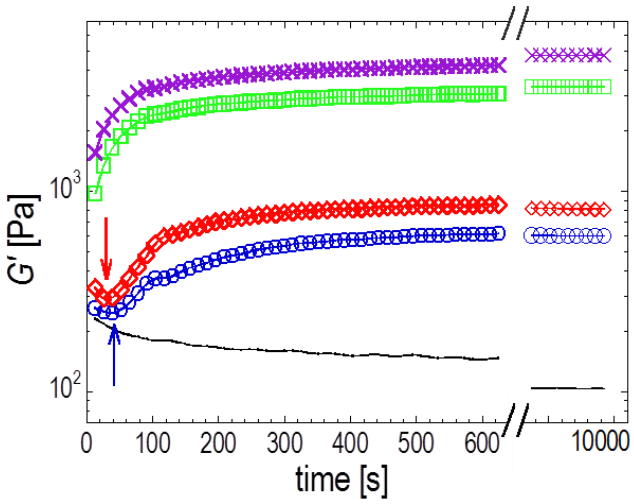

Fig. 4 Time dependence of the elastic modulus at ω=1 rad s^{-1} for the unfilled blend (solid line) and filled blends at Φ=0.16 (circles), 0.22 (diamonds), 0.67 (squares), and 0.91% (crosses).

micrographs of Fig. 5 also support this conclusion. The morphologies of the sample at Φ=0.22% before and after the thermal annealing are compared. The nanoclays, which initially lye on distinct points of the polymer-polymer interface (Fig. 5.a; see also Fig. 1.b), at the end of the annealing result well aligned along the contours of the residual interface (Fig. 5.b-d). High magnification micrographs exclude significant overlapping of the nanoplatelets, which rather seem to touch each other edge to edge. In this configuration, hydroxylated interactions establish between contiguous nanoplatelets,[28] which form a superstructure that spans over the entire polymer-polymer interface. Further phase coarsening is hindered as it would imply energetically costly processes, such as detaching of the particles from the interface, bending of the clay stacks, or disruption of the network. The degree of morphology stabilization increases with the extent of coverage of the initial polymer-polymer interface. When the filler content is high enough, the particles saturate the initial interface and the morphology cannot evolve during time. According to Fig. 3, this condition is achieved at some Φ between 0.36 and 0.67%. The morphology of the as-prepared sample at Φ=0.67% is shown in Fig. 6. The particles indeed cover the entire initial interface, confirming that interfacial saturation is the requisite to achieve full morphology stabilization. Alternatively, phase coarsening proceeds until the strength of the interfacial structure induced by the crowding of nanoclays offsets the interfacial tension. The stress-bearing ability of the interfacial network, ultimately responsible for the stability of the co-continuous structure, is studied in the next section through viscoelastic analysis.

Elasticity and structure of the interfacial particle network

Rheological analysis provides valuable information on the elasticity and structure of percolating networks of nanoparticles embedded in host polymer matrices. Small amplitude frequency scans were performed at the end of time

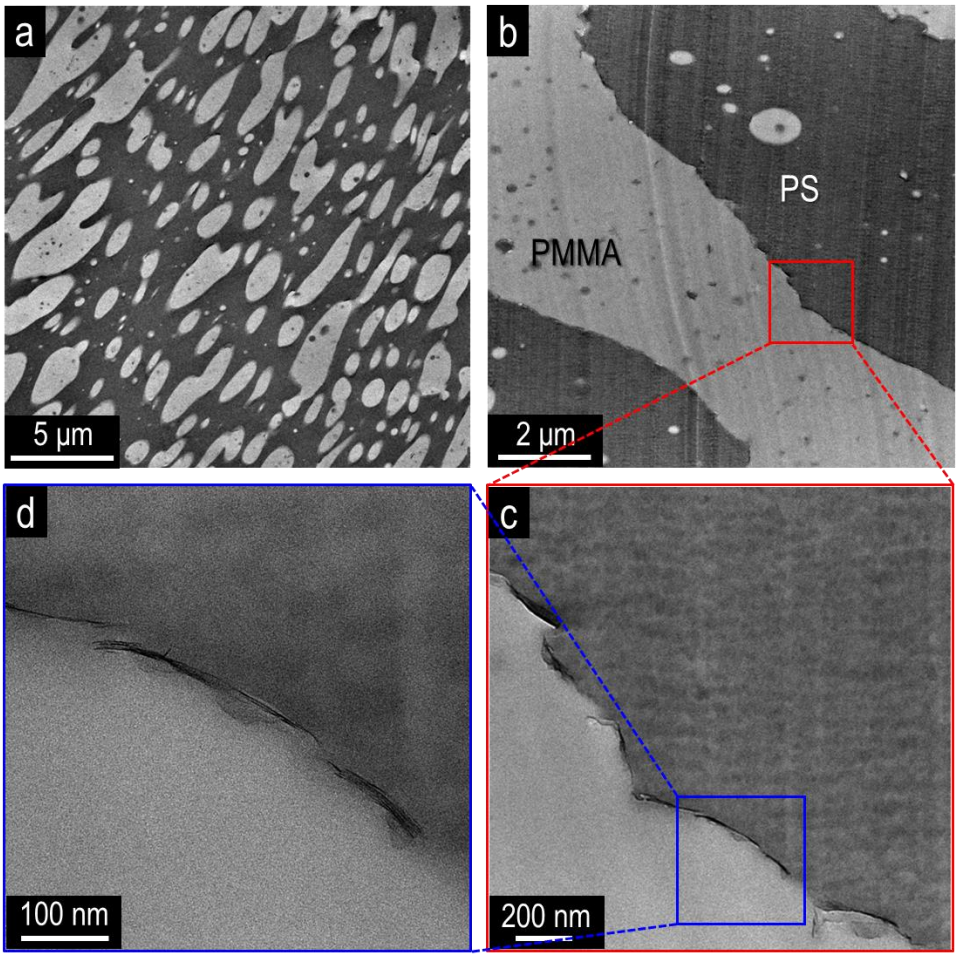

Fig. 5 TEM micrographs showing the microstructure of the sample at Φ=0.22 vol%: (a) as-prepared; (b-d) after 3-hours annealing at T=215°C. The bright and dark phases are PMMA and PS, respectively.

sweep experiments, i.e. when the interfacial network of nanoparticles was formed and the blend morphology was fully evolved. The dynamic moduli are shown in Fig. 7. The unfilled blend exhibits the typical behaviour of co-continuous blends, characterized by a deviation from the terminal behaviour of single phase polymer melts ($G'(\omega\rightarrow 0)\sim\omega^2$ and $G''(\omega\rightarrow 0)\sim\omega^1$). In particular, the low-frequency elastic modulus scales with frequency as $G'\sim\omega^{0.7}$, while the effect on G'' is negligible. We now focus on the effect of the nanoparticles. Hereinafter we restrict our attention to G', which is much more sensitive than G'' to the presence of the filler. The nanoclays at the polymer-polymer interface cause a remarkable increase of G' at low frequency. The scaling law remains power law-like, but the exponent α decreases with filler content, becoming negligible at $\Phi\geq 0.67\%$ (see inset of Fig. 7.a). This behaviour reminds that of nanocomposites based on single polymer matrix, whose relaxation dynamics arrest above the filler percolation threshold, Φ_c. In such conditions, the behaviour of the nanocomposite is dominated by the elastic particle network, and a descriptive two-phase model can be used to isolate its contribution and studying it separately.[29] The two-phase model provides an approximation of the complex viscoelastic behaviour of polymer nanocomposites above Φ_c, in which two

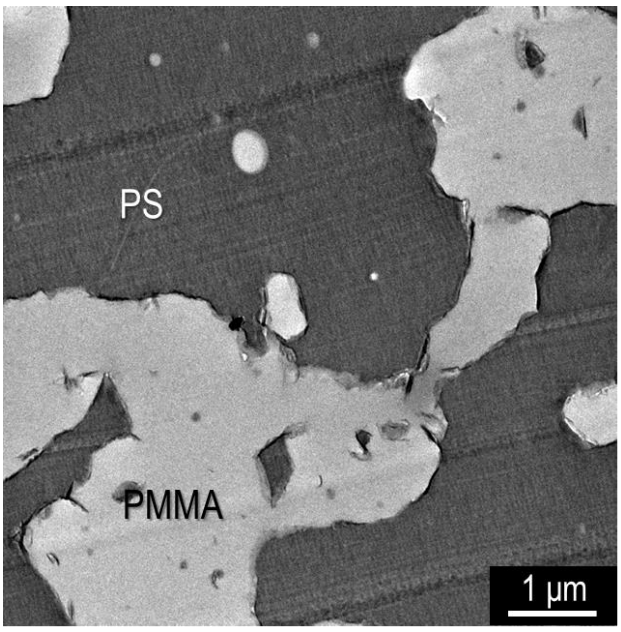

Fig. 6 Microstructure of the as-prepared sample at Φ=0.67%.

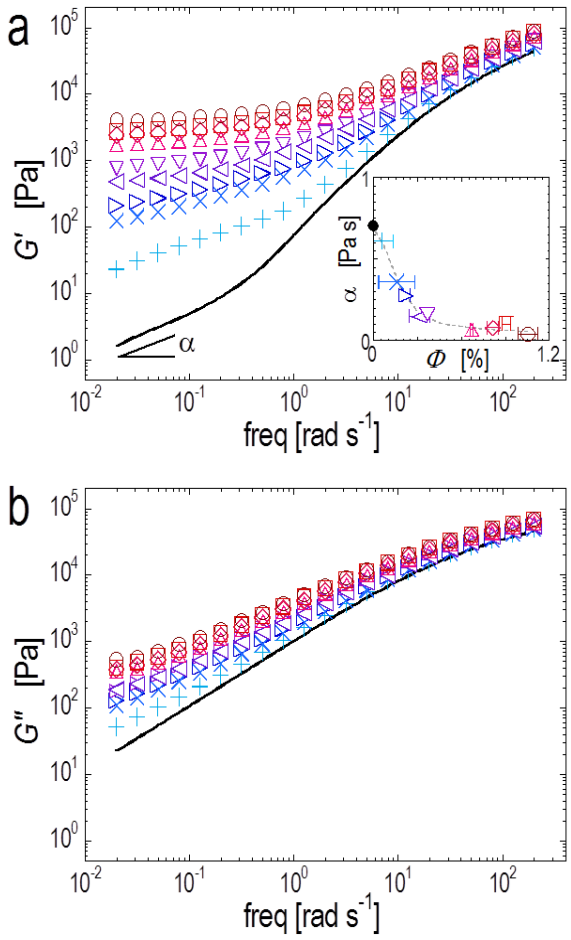

Fig. 7 Elastic (a) e viscous (b) modulus as a function of frequency for the unfilled blend (solid line) and the filled samples at Φ=0.06 (plus), 0.16 (cross), 0.22 (right arrow), 0.31 (left arrow), 0.36 (reverse triangle), 0.67 (triangle), 0.81 (diamond), 0.91 (square), and 1.06% (circle). The inset in (a) shows the power-law exponents of the low-frequency dependence of the moduli.

well distinct dynamical families can be identified: the predominantly viscous polymer matrix and the basically elastic particle network. The validity of this assumption is proved through the building of a master curve of $G'(\omega)$ of samples at different $\Phi>\Phi_c$. Only two shift factors, each one with a precise physical meaning, are used for this purpose: a vertical shift factor, b_Φ, which represents the Φ-dependent network elasticity, and an horizontal shift factor, a_Φ, which is the frequency that separates the regime in which the behaviour is dominated by the particle network ($\omega<a_\Phi$) to that in which the polymer governs the macroscopic response ($\omega>a_\Phi$). The two-phase model was already proved to be able to describe the viscoelasticity of a wide variety of polymer nanocomposite,[29] including polymer blends with drop-in-matrix morphology.[25] Here we exploit it to isolate the contribution of the interfacial particle network from that of the host matrix. Such an approach is essential in the case of co-continuous blends, whose inherent elasticity could mask that of the nanoparticles at low filler contents. To face this problem, first we build the master curve of G' starting from the samples at high filler contents, for which the network elasticity can be clearly identified (here the samples at $\Phi\geq$0.67%). Once the master curve is available, we scale on it the G' curves of the samples at lower Φ. The elasticity of the tenuous interfacial particle network which forms in these samples is thus given by the vertical shift factor b_Φ coming out from the scaling procedure. The step-by-step procedure for scaling the G' curves is described in detail elsewhere[30] and it is reported here as ESI† (Section S2). The resulting master curve is shown in Fig. 8. The building of the master curve also allows to confidently identify all the samples above Φ_c. This can be done considering that the strict interrelationship between the horizontal and vertical shift factors implies the impossibility of scaling G' curves of samples below Φ_c unless violating the physical constraints of the two-phase model.[31] As a result, Φ_c can be sought in the Φ-range between the last non-scalable curve and the first scalable one. The overlay of the scaled G' curves of samples at $\Phi\geq$0.22% is excellent, while the G' curves of samples at $\Phi<$0.22% are not scalable (see inset of Fig. 8). Accordingly, the Φ_c of our system falls between 0.16 and 0.22%. The estimate of Φ_c is carried out in the next Section. Here we limit the attention to the samples at $\Phi\geq$0.22%, whose scaled G' curves nicely overlap revealing the relaxation dynamics of the interfacial network of nanoparticles. Remarkably, the master curve is perfectly superimposed to those obtained in a previous work[25] for systems based on the same polymers and nanoparticles as used here, but in which the matrix was either pure PS or a PS/PMMA blend with drop-in-matrix morphology (Fig. 9). This means that the way in which the relaxation dynamics arrest because of the filler network does not depend on the microstructure of the host matrix. Nevertheless, in the next Section we show that the morphology of the matrix is crucial in determining the space arrangement of the nanoparticles within the network, substantially affecting its structure and elastic properties.

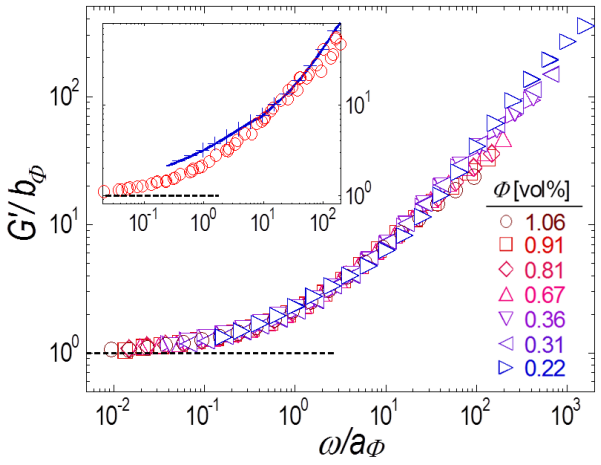

Fig. 8 Master curve of G' built by scaling the G' curves of samples at $\Phi\geq$0.22% (see Supporting Information). Symbols and colors are the same as in Fig. 7. The inset shows the non-scalability of the curve at Φ=0.16% (cross) on the master curve obtained from all the samples at $\Phi\geq$0.22% (circles).

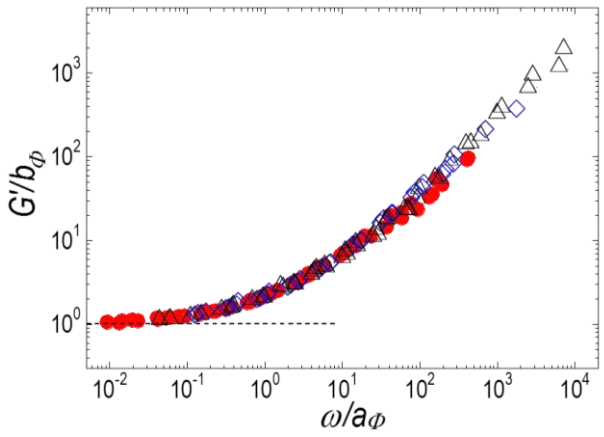

Fig. 9 Overlay of the master curve of G' of the co-continuous samples studied in this work (same as in (a); full circles) and those of samples based on pure PS (empty triangles) and on PS/PMMA blend (85/15 wt/wt) with drop-in-matrix morphology (empty diamonds) taken from ref. 25.

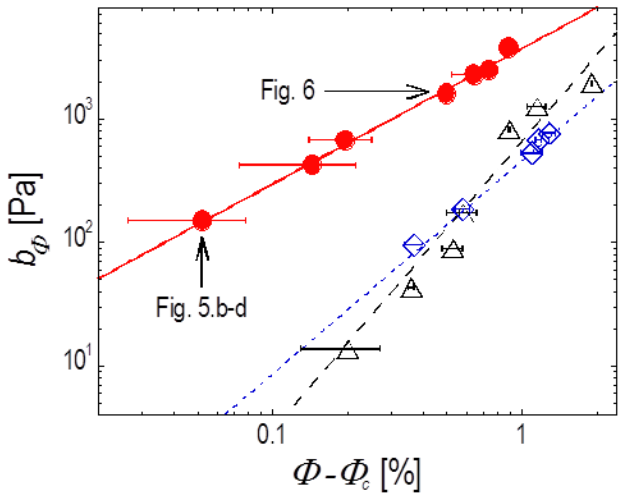

Fig. 10 Network elasticity as a function of reduced filler content (full circles) and power-law fitting to the experimental data (solid line). The data and corresponding fitting lines for systems based on pure PS (empty triangles) and a PS/PMMA blend (85/15 wt/wt) with drop-in-matrix morphology (empty diamonds) are reported for comparison (data from ref. 25).

Percolation approach and structure of the interfacial particle network

The elasticity of particle networks just above Φ_c scales with filler content as $G'_0=k(\Phi-\Phi_c)^v$, where k is a measure of the strength of the network ($k=G'_0$ at $\Phi-\Phi_c=1$), and v is a constant related to the stress bearing mechanism.[32] The low-frequency plateau of the G' curves provides a rough estimate of the network elasticity, since $G'_0=G'(\omega\rightarrow0)$. Rather than using extrapolation procedures, here we refer to the vertical shift factors used to build the master curve of Fig. 8, which represents the network elasticity. Plotting b_Φ versus the reduced filler content, $\Phi-\Phi_c$, and fitting a power-law to the data provides a reliable estimate of Φ_c as the value that returns the highest regression coefficient.[30] The result of this procedure is shown in Fig. 10.a. The best power-law fitting to the experimental data (full circles) was obtained by setting Φ_c=0.17%, which leads to k=3779 ± 660 and v=1.09 ± 0.29. The same procedure was previously applied to systems based on the same polymers and nanoparticles as used here, but in which the matrix was either pure PS or a drop-in-matrix PS/PMMA blend (85/15 w/w).[25] Datasets and fitting lines are shown in Fig. 10.a for comparison. The fitting parameters of the three systems are summarized in Table 1. The comparison enables us to elucidate the role of the matrix in dictating the space arrangement of the nanoparticles.

Table 1 Percolation thresholds and fitting parameters.

Matrix	Φ_c [%]	k [Pa]	v
Co-continuous blend (this work)	0.17	3779 ± 660	1.09 ± 0.29
Single polymer (pure PS)[25]	0.76	656 ± 26	2.34 ± 0.36
Drop-in-matrix blend (PS/PMMA 85/15 w/w)[25]	0.95	457 ± 5	1.73 ± 0.17

The value of Φ_c found in case of co-continuous matrix is considerably lower than that obtained when the particles are dispersed in pure PS, which in turn is lower than that in the PS-PMMA blend with drop-in-matrix morphology. The previous ranking can be easily explained by accounting for the inclination of the nanoplatelets to gather at the polymer-polymer interface: when the blend exhibits co-continuous morphology, the particles are forced to align along a continuous path, thus percolating at low contents; in contrast, when drop-in-matrix blends are considered, the nanoplatelets accumulate in the proximity of isolated domains, and higher amount of particles are required to generate a continuous path.[25] Now we consider the elastic features of the interfacial network of nanoparticles which forms in the co-continuous blend. The data in Fig. 10 and Table 1 reveal that the strength of the network in the co-continuous matrix is significantly higher than that of the networks that the same nanoparticles form in pure PS or in the blend with drop-in-matrix morphology. The difference is particularly pronounced at low reduced filler content. This experimental evidence can be explained in the light of the different structures of the networks in the three systems. Schematics inspired by the TEM analyses carried out here and in ref. 25 are shown in Fig. 11.a. In the co-continuous blend, large volumes of sample are precluded to the particles, which are forced to lie on the polymer-polymer interface. Such a configuration minimizes the probability of isolated nanoparticles and agglomerates, which are not effective in bearing the stress. In addition, strong edge-to-edge interactions are predominant respect to the case of homogeneous PS matrix or in blends with drop-in-matrix morphology (Fig. 11.a vs. Fig. 11.b or c). On the other hand, the comparison between the critical exponents v reveals that an incremental addition of nanoparticles above Φ_c has a minor effect in case of co-continuous matrix. To investigate the

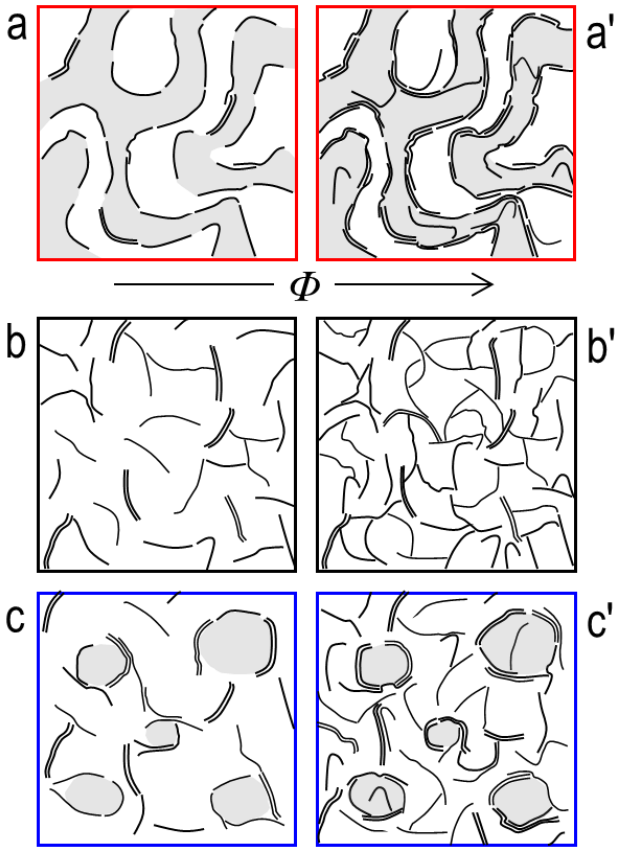

Fig. 11 Sketches showing the space arrangement of the filler in the co-continuous blend (a, a'), homogeneous matrix (b, b') and drop-in-matrix blend (c, c').

strengthening mechanism of the interfacial network with the increase in filler content, we refer to the expression of the elastic modulus of a nanoplatelet-coated polymer-polymer interface of a co-continuous blend, G'_{int}, derived by Macosko and co-workers:[33]

$$G'_{int} = \frac{C \cdot K_{int}}{t^m} \cdot \frac{t^w}{\xi} \qquad (1)$$

where C is a constant, K_{int} is the compressive modulus of the particle monolayer from interfacial rheology, t^w, is the average thickness of the walls of the filler network, and t^m is the thickness of the particle monolayer. According to Eq. 1, the strengthening of the interfacial network arises from the increase of the ratio t^w/ξ. Since in the studied systems ξ rapidly approaches a limiting lower value (see Fig. 3), we conclude that the network strengthens with Φ mostly because of a thickening of the network branches. To test this hypothesis, the distributions of the thicknesses of the network walls were estimated for two samples at low and high filler content, and the calculated values of t^w were used to derive the theoretical values of the network strength by means of Eq. 1 (calculations are provided as ESI†, Section S3). The results summarized in Fig. 12 confirm that the average thickness of the interfacial structure increases from t^w~9 nm (Φ=0.22%) to t^w~14 nm (Φ=0.67%); and the excellent quantitative agreement between

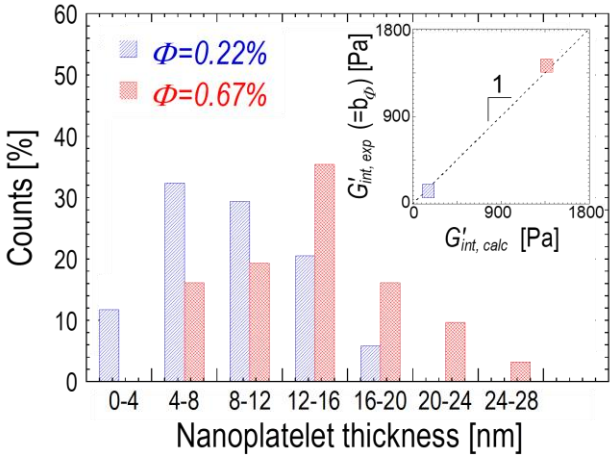

Fig. 12 Size distribution of the wall thickness of the nanoplatelet network in the co-continuous blends filled at Φ=0.22% and 0.67%. The experimental value of the elasticity of the interfacial network ($G'_{int,\ exp}$) is reported in the inset as a function of the value calculated via Eq. 1 ($G'_{int,\ calc}$).

calculated and experimental values of G'_{int} (inset of Fig. 12) corroborates the robustness of our analysis.

If the interfacial network in the co-continuous matrix mainly strengthens due to the thickening of its branches (Fig. 11.a vs. 11.a'), the reinforcing mechanisms is different when the host matrix is a single polymer phase. In this case, the added particles are free to randomly insert themselves into the pre-existing network due to the absence of a preferred polymer-polymer interface. As a result, each incremental addition of particles potentially generates new effective particle-particle contacts (Fig. 11.b vs. 11.b'). This increases the stress bearing ability of the network, reflecting in a high value of v. It is not surprising to find out that the blend with drop-in-matrix morphology, in which a fraction of ineffective particles accumulates in the proximity of isolated droplets, places between the two extremes of single matrix and co-continuous blend (Fig. 11.c vs. 11.c').

Conclusions

The effects of small amounts ($\Phi \leq 1.06$ vol%) of nanoclay in a co-continuous blend of PS and PMMA was studied. The filler selectively locates at the polymer-polymer interface, thus promoting a drastic decrease of the characteristic size of the polymer phases in the as-prepared samples. The extent of refinement is proportional to the filler content at low filler content ($\Phi \leq 0.36$%), while further additions of particles have a negligible effect on the size of the polymer phases. On the other hand, the refinement induced at $\Phi \leq 0.36$% is not permanent, and these samples experience noticeable phase coarsening during annealing at high temperature (T=215°C). In contrast, full morphology stabilization was found at $\Phi \geq 0.67$%. A combination of rheological and morphological analyses proves that phase coarsening takes place in the very early stages of the annealing, eventually causing the interfacial crowding of the nanoparticles. The resulting interfacial

structure prevents from further evolution of the polymeric domains. The full morphological stability achieved in the samples at higher filler contents ($\Phi \geq 0.67\%$) originates from the saturation of the entire polymer-polymer interface in the as-prepared samples. The structure and elasticity of the interfacial network of nanoparticles were investigated by means of linear viscoelastic analysis. The contribution of the filler network was isolated by exploiting a descriptive two-phase model. The relaxation dynamics of the interfacial network of nanoparticles were found to be very similar to those of reference systems based on pure PS and a PS/PMMA blend with drop-in-matrix morphology. On the other hand, the structure and elasticity of the particle network in the co-continuous blend are noticeably different from those of the reference systems. In particular, the selective accumulation of the particles at the polymer-polymer interface results in lower filler percolation threshold ($\Phi_c = 0.17\%$) and higher overall elasticity. Both results are a direct consequence of the peculiar space arrangement of the filler, whose alignment along the continuous polymer-polymer interface minimizes the probability of isolated particles and promotes strong edge-to-edge interactions. At the same time, the confinement of the nanoparticles brings about a low sensitivity of the network elasticity to the filler content. Indeed, once the interface is saturated there is no way to accommodate additional particles, which accumulate and form thicker branches without effectively contributing in strengthening the pre-existing network.

References

1 Ramsden, *Proc. R. Soc. London*, 1903, **72**, 156-164.
2 S. U. Pickering, *J. Chem. Soc. Abstr.*, 1908, **91**, 2001-2021.
3 P. S. Clegg, *J. Phys.: Condens. Matter*, 2008, **20**, 113101.
4 A. Taguet, P. Cassagnau and J. M. Lopez-Cuesta, *Prog. Polym. Sci.*, 2014, **39**, 1526–1563.
5 M. Salzano de Luna and G. Filippone, *Eur. Polym. J.*, 2016, **79**, 198–218.
6 C. W. Macosko, *Macromol. Symp.*, 2000, **149**, 171-184.
7 X. Q. Liu, R. H. Li, R. Y. Bao, W. R. Jiang, W. Yang, B. H. Xie and M. B. Yang, *Soft Matter*, 2014, **10**, 3587−3596.
8 J. M. Feng, X. Q. Liu, R. Y. Bao, W. Yang, B. H. Xie and M. B. Yang, *RSC Adv.*, 2015, **5**, 74295−74303.
9 E. J. Dil, N. Virgilio and B. D. Favis, *Eur. Polym. J.*, 2016, **85**, 635–646.
10 E. Cohen, L. Zonder, A. Ophir, S. Kenig, S. McCarthy, C. Barry and J. Mead, *Macromolecules*, 2013, **46**, 1851–1859.
11 A. Nuzzo, S. Coiai, S. C. Carroccio, N. T. Dintcheva, C. Gambarotti and G. Filippone, *Macromol. Mater. Eng.*, 2014, **299**, 31–40.
12 Z. Zhang, S. Wang, J. Zhang, W. Zhu, X. Zhao, T. Tian and T. Chen, *Chem. Eng. J.*, 2016, **285**, 439–448.
13 M. Salzano de Luna, M. Galizia, J. Wojnarowicz, R. Rosa, W. Lojkowski, C. Leonelli, D. Acierno and G. Filippone, *Express Polym. Lett.*, 2014, **8**, 362–372.
14 L. Imperiali, C. Clasen, J. Fransaer, C. W. Macosko and J. Vermant, *Mater. Horiz.*, 2014, **1**, 139-145.
15 M. N. Lee and A. Mohraz, *Adv. Mater.*, 2010, **22**, 4836-4841.
16 L. Bai, J. W. Fruehwirth, X. Cheng and C. W. Macosko, *Soft Matter*, 2015, **11**, 5282–5293.
17 G. Filippone and D. Acierno, *Macromol. Mater. Eng.*, 2012, **297**, 923−928.
18 M. Si, T. Araki, H. Ade, A. L. D.Kilcoyne, R. Fisher, J. C. Sokolov and M. H. Rafailovich, *Macromolecules*, 2006, **39**, 4793-4801.
19 J. S. Hong, H. Namkung, K. H. Ahn, S. J. Lee and C. Kim, *Polymer*, 2006, **47**, 3967−3975.
20 J. Huitric, J. Ville, P. Médéric, M. Moan and T. Aubry, *J. Rheol.*, 2009, **53**, 1101−1119.
21 S. Vandebril, J. Vermant and P. Moldenaers, *Soft Matter*, 2010, **6**, 3353−3362.
22 I. Labaume, P. Médéric, J. Huitric and T. Aubry, *J. Rheol.*, 2013, **57**, 377−392.
23 M. Trifkovic, A. T. Hedegaard, M. Sheikhzadeh, S. Huang and C. W. Macosko, *Macromolecules* 2015, **48**, 4631–4644.
24 S. Huang, L. Bai, M. Trifkovic, X. Cheng and C. W. Macosko, *Macromolecules*, 2016, **49**, 3911−3918.
25 G. Filippone, A. Causa, M. Salzano de Luna, L. Sanguigno and D. Acierno, *Soft Matter*, 2014, **10**, 3183−3191.
26 E. M. Herzig, K. A. White, A. B. Schofield, W. C. K. Poon and P. S. Clegg, *Nat. Mater.*, 2007, **6**, 966.
27 M. E. Cates and P. S. Clegg, *Soft Matter*, 2008, **4**, 2132−2138.
28 S. Sinha Ray, K. Okamoto and M. Okamoto, *Macromolecules*, 2003, **36**, 2355−2367.
29 G. Filippone and M. Salzano de Luna, *Macromolecules*, 2012, **45**, 8853−8860.
30 G. Filippone, G. Romeo and D. Acierno, *Langmuir*, 2010, **26**, 2714−2720.
31 G. Filippone, M. Salzano de Luna, D. Acierno and P. Russo, *Polymer*, 2012, **53**, 2699−2704.
32 D. Stauffer and A. Aharony, *Introduction to Percolation Theory*, Taylor & Francis, London, 1992.
33 L. Bai, S. He, J. W. Fruehwirth, A. Stein, C. W. Macosko and X. Cheng, *J. Rheol.*, 2017, **61**, 575-587.